EXPERIMENTAL AND COMPUTATIONAL STUDY OF Co(II), Ni(II), Cu(II) AND Zn(II) COMPLEXES WITH THE AZO DYE DERIVED FROM 2-AMINO-4-METHYL PYRIDINE AND β-NAPTHOL

Satya Narayan Chaulia
G.M. University – India

Abstract. A series of metal complexes of Co(II), Ni(II), Cu(II) and Zn(II) complexes with the azodye ligand derived from the 4-methyl-2-aminopyridine and β-napthol have been synthesised. These complexes and the ligand have been characterised by analytical and spectral techniques such as IR, NMR, electronic and magnetic measurement. The structural compositions of the ligand and complexes have been determined by FAB-MS structural studies. The computational study of studied compounds has been made to determine geometrical parameters and electronic parameters. The experimental data of the compounds are compared with the computationally generated data. The structural activity relationships of all the compounds have been computed to explain their biological properties.

Keywords: metallochromic reagents; computational study; correlation coefficient, MEP study

Introduction

Azo dye and its first row transition metal complexes having nitrogen and oxygen donor atoms have been studied extensively by the scientific community. These systems show marked biological properties such as antibacterial, antiviral, antihelminthes (Adsule et al., 2006). These are also used extensively not only in the dye industry but also as the analytical and metallochromic reagents (Guha et al., 2000; Hallas & Choi, 1999). Metal complexes derived from heterocyclic amines have been widely investigated for their applications in the field of medicine, catalysis and great variety of biological activities such as antimalarial, antibacterial, antiviral agents (Galić et al.,1997). Keeping in mind of this, synthesis and characterisation of a new ligand derived from 2-amino-4-methylpyridine and its metal complexes have been reported.

Materials and methods

All the solvents, the metal salts and other chemicals used are of either analytical grade or high purity supplied by Merck and BDH. Elemental analysis of the ligand and complexes was carried out by Perkin–Elmer elemental analyser, cobalt, nickel, copper contents was determined by Perkin –Elmer2380 atomic absorption spectroscopy and chloride contents was estimated by standard procedure, the molar conductance was measured on an Elico CM conductivity meter using 10^{-3}M in DMF. Magnetic susceptibility of the complexes was measured by Guoy´s balance using $Hg[Co(NCS)_4]$ as a calibrant at room temperature and diamagnetic correction have been made by pascal's constants, IR spectra of the ligand and metal complexes were recorded on using KBr pellets by Perkin Elmer FT- IR spectrometer within the range 4000- 450 cm^{-1}, UV-Visible spectra of the complexes were collected using a THERMO SPECTRONIC 6 HEXIOS α ,^{1}H NMR spectra of the ligand and the Zn(II) complex were obtained from Bruker AV III 500 MHZ FT NMR spectrometer using TMS as reference. FAB-MS spectral study was made on a JEOL SX 102/ DA-6000 mass spectrometer

Computational strategy

All calculations for the metal complexes and the free ligand were performed by employing quantum chemical approach with Becke three parameter hybrid method (Becke, 1993) using the Lee-Yang-Par correlation functional with the 3-21G (d, p) basis set.

Synthesis of the ligand

The ligand as given in the Fig. 1 was synthesised by the coupling reaction between the diazonium chloride derived from the heterocyclic amine and the aromatic hydroxyl compound. The diazonium chloride was prepared by dissolving gram 2-amino-4-methylpyridine in hydrochloric acid, cooled to $0 – 5^0$C and mixed with ice-cooled sodium nitrite solution. The diazonium chloride solution was mixed with ice cooled alkaline solution containing 0.84 gram of β-napthol. The reacting mixture was kept for two days, and then the precipitate was filtered and dried in vacuum. The azo compound was repeatedly recrystallized from the DMF solution.
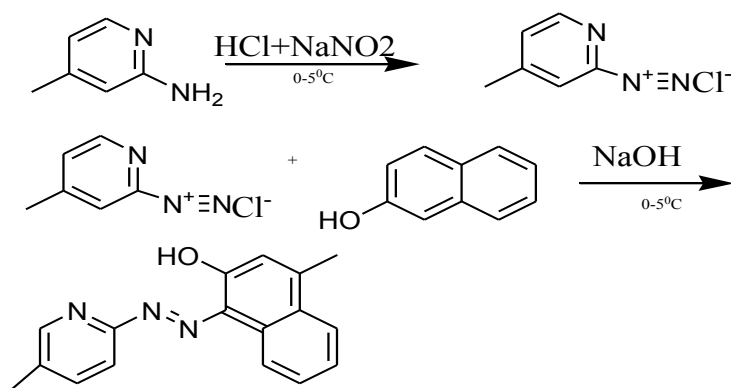
Figure 1. Reaction scheme for the synthesis of the ligand

Synthesis of the metal complexes

The metal chlorides in ethanol were mixed separately with DMF solution of the ligand in 1:2 molar ratio and the resulting solutions were heated to 60^0C for about an hour on a heating mantle. The solution was then cooled down to room temperature and the, concentrated ammonia solution was added drop by drop with stirring till the formation of a neutral solution. The solid complexes which are given in the Fig. 2 thus separated were then washed with ethanol, followed by ether and dried in vacuum.
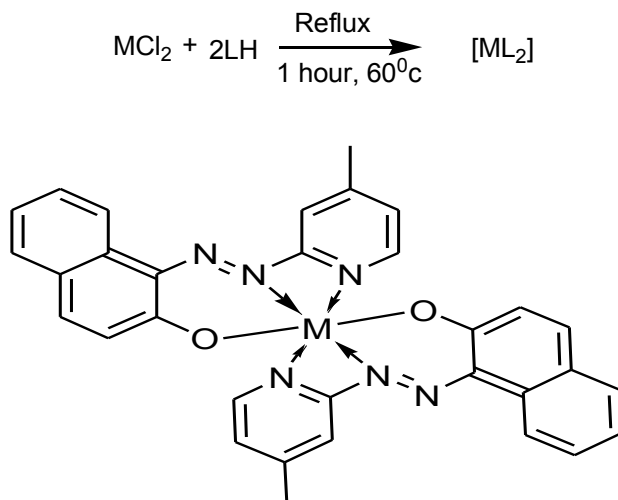

Figure 2. Structure of the metal complexes

Results and discussion

Analytical study

It has been found from the analytical data (Table 1) that the molar ratio of the metal to the ligand was found to be 1:2 and formula of the metal complexes agreed well with the general formula $[ML_2]$, where M represents Co(II), Ni(II), Cu(II) and M= Zn(II).

L is the deprotonated azo ligand. The complex compounds were found to be non-electrolyte in nature as DMF solution of the metal compounds showed low conductance. All the compounds are stable with sharp melting points indicating purity of the substance.

Table 1. Analytical data

| Compound	Colour	Yield(%)	M.P (^{0}C)	% Found (calcd)			
				M	C	H	N
1	Reddish Brown	58	70	-	72.89 (72.99)	4.92 (4.98)	15.87 (15.96)
2	Brick red	40	>300	10.08 (10.10)	65.82 (65.87)	4.05 (4.15)	14.37 (14.40)
3	red	45	>300	10.01 (10.06)	65.82 (65.89)	4.09 (4.15)	14.39 (14.41)
4	grey	47	>300	10.76 (10.80)	65.29 (65.35)	3.98 (4.11)	14.19 (14.29)
5	Brown	42	>300	14.22 (14.25)	65.11 (65.15)	4.07 (4.10)	14.21 (14.25)

IR study

The mode of bonding between the ligand and the metal complexes was examined by comparing IR spectra of the ligand as given in the Graph 1 and metal complexes as given in the Graph 2. The IR spectrum of the ligand gives a broad band at 3442 cm^{-1} due to stretching vibration of the naphthyl (O-H) group, this peak is missing from the spectra of the complexes due to the absence of absorption bands associated with –OH stretching. This indicates deprotonation of the naphthyl –OH group upon complexation and bonding of the metal ion with the oxygen atoms of the naphthyl –OH group. This observation is supported by the shifting of the v(C-O) band observed in the ligand at 1277 cm^{-1} to ~ 1249 cm^{-1} in the metal complexes (Saxena & Tondon, 1984). The ligand shows a band at 1512 cm^{-1} due to the vibration of $-N = N - -N = N -$ group but this band is shifted to ~ 1458 cm^{-1} in the metal complexes, this fact suggests the bonding of the azo nitrogen with the

metal ion (King & Bisnette, 1966). In the IR spectrum of the ligand, a band is observed at 1620 cm^{-1} due to the vibration of(C=N) group and this band is shifted to ~ 1592 cm^{-1} this indicates bonding of pyridine nitrogen with the metal ions (Anitha et al, 2012). The lower region of the metal complexes also depicts two bands at ~508 cm^{-1} and ~489 cm^{-1} due to the vibration of (M-N) bond and (M-O) bond respectively, this observation indicates bonding of the metal ion with the nitrogen atom of the azo group and oxygen atom of the napthyl group (Nakamato, 2009).
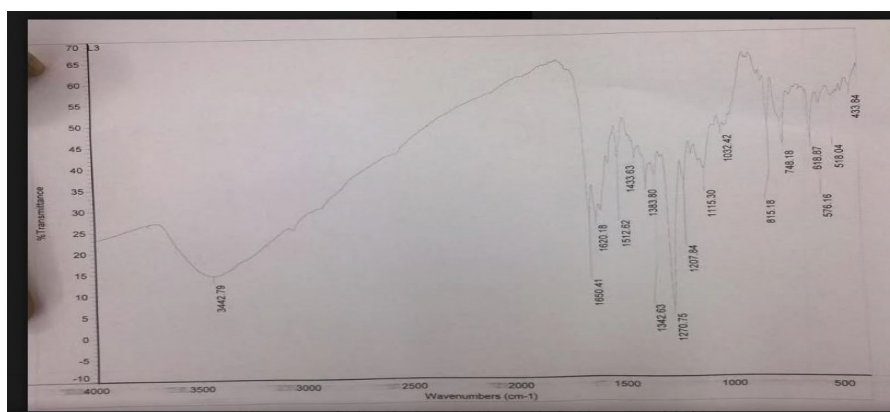

Graph 1. IR spectrum of the ligand
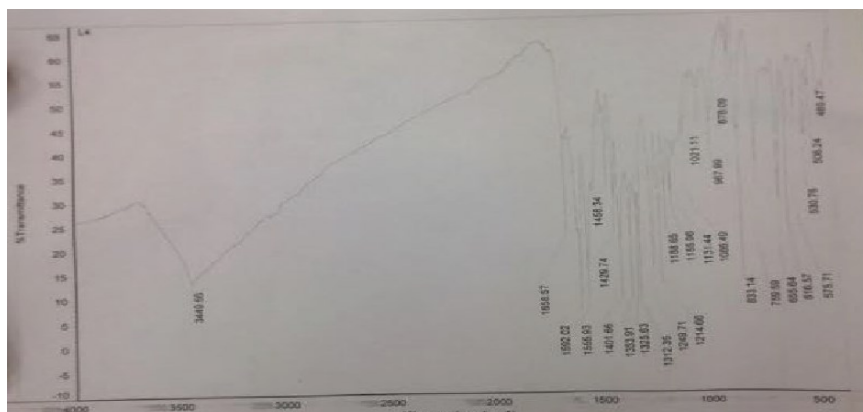
Graph 2. IR spectrum of the Ni(II) complex

The vibrational spectral data of the ligand and its complexes were computed by using the force field AM1 and PM3 force fields and the data were compared with the experimental data(Table 2). Semi-empirical method using the force fields

AMI and PM3 were used as they give good correlation between experimental and computational data. The vibration frequencies of the ligand and Ni(II) complex as collected experimentally were plotted in the form of graphs verses the computationally generated frequencies using the force field AM1 (Graphs 3 and 5) and PM3 (Graphs 4 and 6). The experimental data are in good agreement with the computational data for the ligand and metal complex with the correlation coefficient values are ~0 .99.
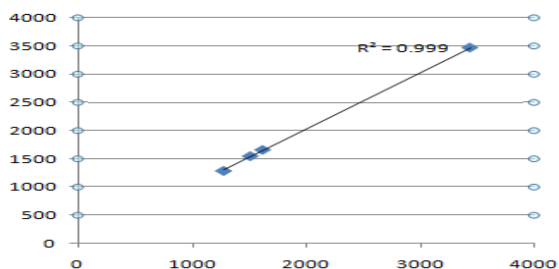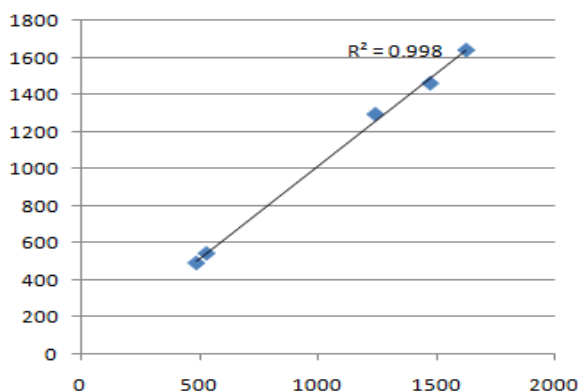

Graph 3. Experimental frequencies vs. calculated frequencies of the ligand(AM1)
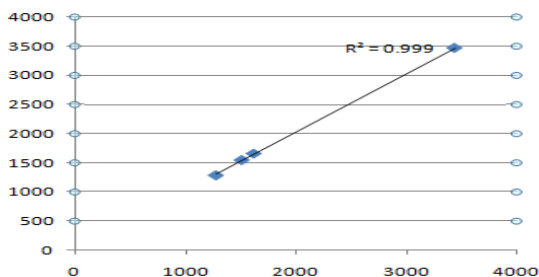
Graph 4. Experimental frequencies vs. calculated frequencies of the ligand(PM3)
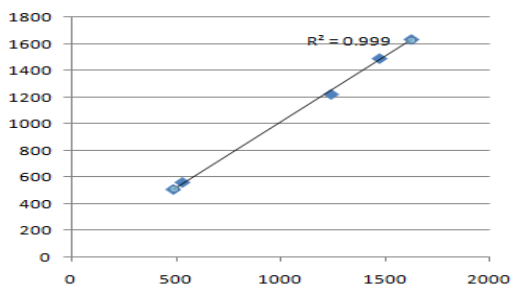
Graph 5. Experimental frequencies vs. calculated frequencies of the Ni(II) complex(AM1)

Graph 6. Experimental frequencies vs. calculated frequencies
of the Ni(II) complex(PM3)

Table 2. Experimental and computational vibration frequency data of the ligand

Band	EXPT v/cm-1	AM1 v/cm^{-1}	Intensity	PM3 v/cm^{-1}	Intensity
(C-O)	1243	1290	0.253	1277	8.50
(C=N)	1620	1662	66.20	1628	45.47
(N=N)	1512	1551	18.23	1524	18.31
(O-H)	3442	3469	42.96	3844	13.56

Electronic spectra and magnetic measurement study

The electronic and magnetic measurement study was made to establish the geometry of the complex compounds as we failed to synthesise single crystals of complex compounds. The electronic spectra of the ligand as given in the Graph 7 and its complexes were recorded in 10^{-3}M of DMF solution and presented in tabular form along with the computational data. The computational data were generated by using the B3LYP level of theory.

The electronic spectrum of the Co(II) complex gives four bands at 13422 cm^{-1}, 19230 cm^{-1} 22727 cm^{-1}, and 37037 cm^{-1} due to $^4T_{1g}(F) \rightarrow ^4T_{2g}(F)$, $^4T_{1g}(F) \rightarrow ^4A_{2g}(F)$, $^4T_{1g}(F \rightarrow ^4T_{2g}(P)$ and CT transitions respectively. These bands indicate distorted octahedral geometry of the Co(II) complex which is supported by magnetic value of the complex (Lever & Solomon, 2014). The electronic parameters of the Co(II) were calculated by using the following equations and given in the Tables 4 and 5.

$$Dq = v2 - v1/10$$

$$B = v2 + v3 - 3\ v1/15$$

$$\beta 35 = B/\ 971$$

$$\beta 35\% = (1 - \beta 35) \times 100$$

Table 3. Experimental and computational vibration frequency data of the Ni(II) complex

Band	EXPT v/cm^{-1}	v/cm^{-1}	AM1 Intensity	v/cm^{-1}	PM3 Intensity
(C-O)	1245	1223	24.41	1294	284.12
(C=N)	1628	1634	34.11	1640	28.41
(N=N)	1476	1491	31.64	1461	323
(M-N)	535	564	6.96	543	3.86
(M-O)	492	511	24.76	491	4.74

Table 4. Electronic spectral data of the ligand and metal complexes

compound	Expt wavelength(nm)	Calcd wavelength(nm)	assignment
Ligand	281	310	$n-\pi*$
	396	410	
$[CoL_2(H2O)_2]$	745	710	$^4T_1g(F) \rightarrow {}^4T_2g(F)$
	520	513	$^4T_1g(F) \rightarrow {}^4A_2g(F)$
	440	428	$^4T_1g(F) \rightarrow {}^4T_2g(P)$
	270	265	CT
$[NiL_2(H2O)_2]$	720	619	$^3A_2g(F \rightarrow {}^3T_2g(F)$
	515	527	$^3A_2g(F) \rightarrow {}^3T_1g(F)$
	434	437	$^3A_2g(F) \rightarrow {}^3T_1g(P)$
	275	257	CT
$[CuL_2(H_2O)2]$	545	574	$^2Eg \rightarrow {}^2T_2g$
	260	270	

The Ni(II) complex also depicts four bands in its spectrum at 13890 cm^{-1}, 19417 cm^{-1}, 23041 cm^{-1} and 36363 cm^{-1} corresponding to $^3A_{2g}(F) \rightarrow \rightarrow^3T_{2g}(F)$, $^3A_{2g}(F) \rightarrow \rightarrow^3T_{1g}(F)$, $^3A_{2g}(F) \rightarrow \rightarrow^3T_{1g}(P)$ and CT transitions respectively. These transitions suggest distorted octahedral geometry of the Ni(II) complex, magnetic measurement of the complex also supports this fact (Shakir et al., 1996). The electronic parameters of the Ni(II) were calculated by using the following equations.

$$Dq = v1/10$$
$$B = v2 + v3 - 3\,v1/15$$
$$\beta 35 = B/1041$$
$$\beta 35\% = (1 - \beta 35) \times 100$$

The Cu(II) complex shows two bands at 35460 cm^{-1} and 18349 cm^{-1}, the band at 38461 cm^{-1} is due to CT band and the band at 16393 cm^{-1} is a d-d band which arises due to $^2E_g \rightarrow \rightarrow {}^2T_{2g}$ transition which favours a distorted octahedral arrangement around the metal ion. The magnetic moment of this compound was found to be 1.24 B.M. which is in the normal range of octahedral symmetry

(Dholakiya & Patel, 2002). The magnetic value of Co(II), Ni(II) and Cu(II) are also within the range of octahedral geometry for the above complexes. The Zn(II) complex is diamagnetic and an octahedral geometry is proposed according to the empirical formula (Dutta & Syamal, 1993).
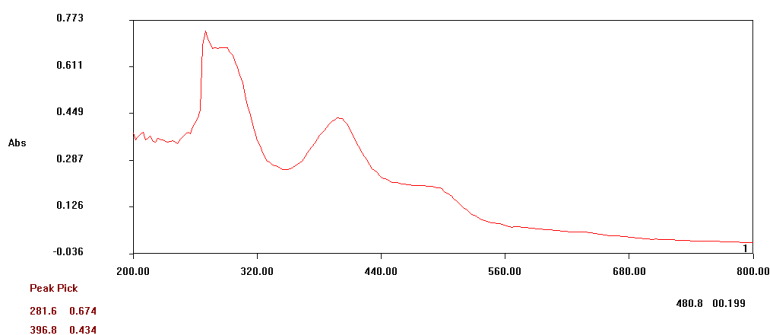

Graph 7. Electronic spectrum of the ligand

The absorption wavelengths of the Co(II) and Ni(II) complexes as collected experimentally were plotted in the form of graphs verses the computationally generated absorption wavelengths (Graphs 8 and 9) using the force field ZINDO. The experimental data are in good agreement with the computational data for the ligand and metal complex with the correlation coefficient values are ~0 .94.
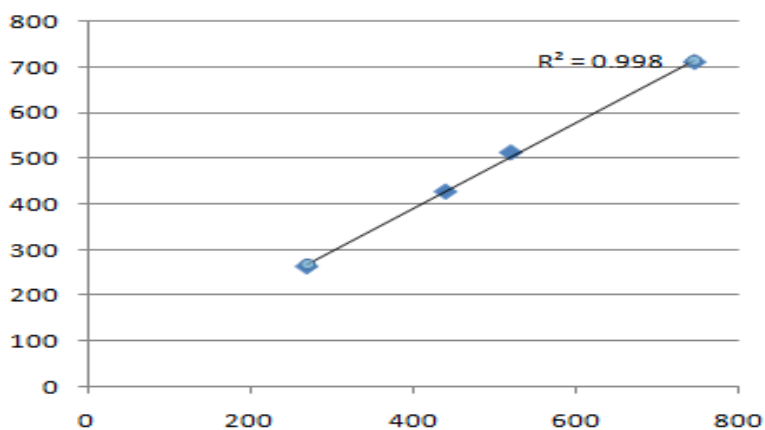
Graph 8. Experimental wavelengths vs. calculated wavelengths of the Co(II) complex
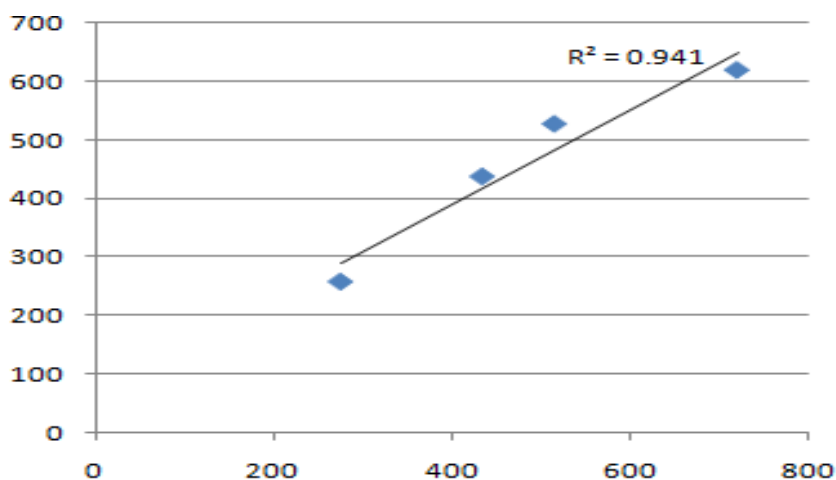
Graph 9. Experimental wavelengths vs. calculated wavelengths
of the Ni(II) complex

Table 5. Electronic parameters of the metal complexes

| compound	B	β_{35}	% of β_{35}	υ_2/υ_1	Geometry	μ_{eff} B.M.
$[CoL_2 H_2O)_2]$	112.7	0.116	88.4	1.43	Distorted octahedral	3.54
$[NiL_2(H_2O)_2]$	52.5	0.050	95	1.397	Distorted octahedral	2.32
$[CuL_2(H_2O)_2]$	-	-	-	-	Distorted octahedral	1.27

NMR study

The ^{1}H NMR study of the ligand and Zn(II) complex as given in the Graphs 10 and 12 in Deuterated DMSO shows signals corresponding to the suggested struc-ture of the ligand and Zn(II) complex. The multiplet appeared in the spectrum of the ligand at δ 7.2-7.9 ppm may be assigned to the aromatic protons. The spectrum also showed signals at δ 2.8 ppm due to presence of $=C-CH_3$ protons. The signal at δ 8.2 ppm may be due to the presence of =CH-. However, a singlet at δ 10.2 ppm may be attributed to the napthyl (OH) protons. The absence of this peak in the spectrum of the Zn(II) complex indicates deprotonation of napthyl (OH) on complexation (Benial et al., 2000). A correlation graph of the ligand as shown in the Graph 12 is plotted between the chemical shifts data collected experimentally and the chemical shifts data gathered computationally as given inthe Graph 11 and it also reflected good result.
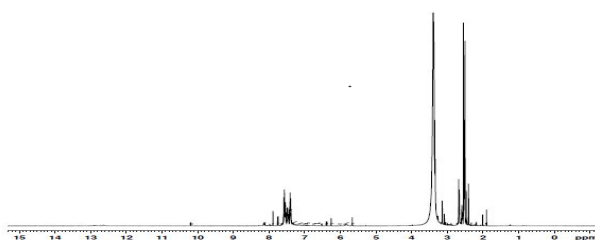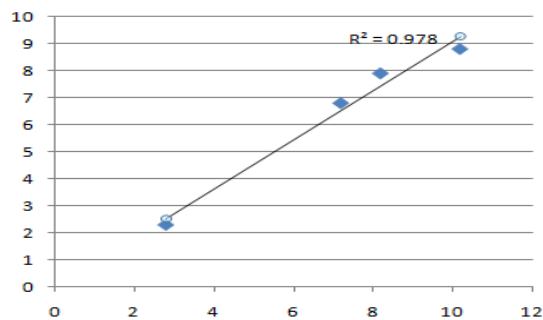
Graph 10. NMR spectrum of the ligand
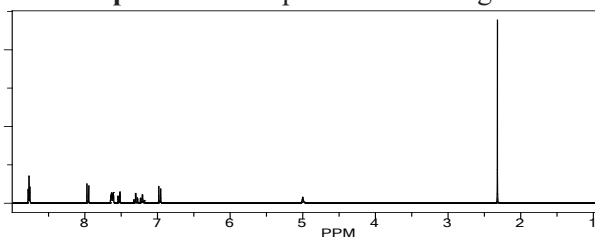
Graph 11. Calculated NMR spectrum of the ligand
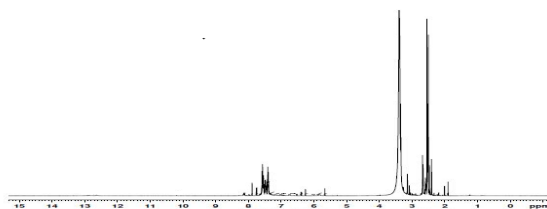
Graph 12. NMR spectrum of the Zn(II) complex

Graph 12a. Experimental chemical shift vs. calculated. chemical shift of ligand

Mass spectra study

The FAB-MS Spectral study of the ligand and its Co(II) complex was made to confirm their structural composition. The FAB-MS spectrum of the ligand shows a peak at 263 m/z corresponding to its molecular mass; it also shows other peaks due to fragmentation of the ligand such as

Figure 3. Fragmentation pattern of the ligand

m/z 235, 211, 185, 132, 94, 66 and 38. The FAB-MS spectrum of the ligand and its fragmentation pattern was given below. The Fragmentation pattern of the ligand confirms the structural composition of the ligand (Figs. 3 and 4).

The FAB-MS spectrum of the Co(II) complex shows a peak at m/z 583 which corresponds to its molecular mass, it also gives other peaks such as m/z 492, 401, 373, 345, 202 and 58 due to its fragmentation which was given below. The different peaks formed in a result of fragmentation also confirm the stoichiometric composition of the complex.

Electrostatic potential map study

The electrostatic potential map(MEP) study of the ligand was made to identify the electrophilic and nucleophilic reactive sites
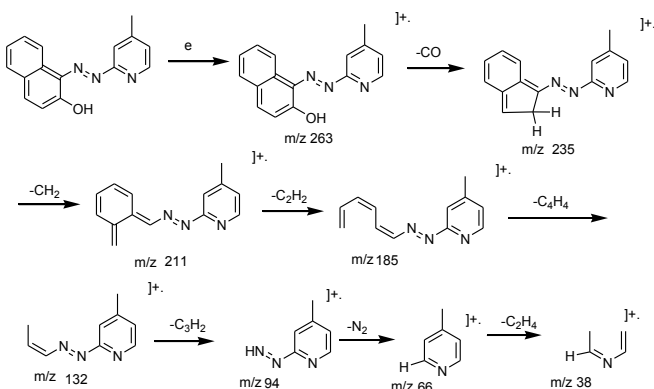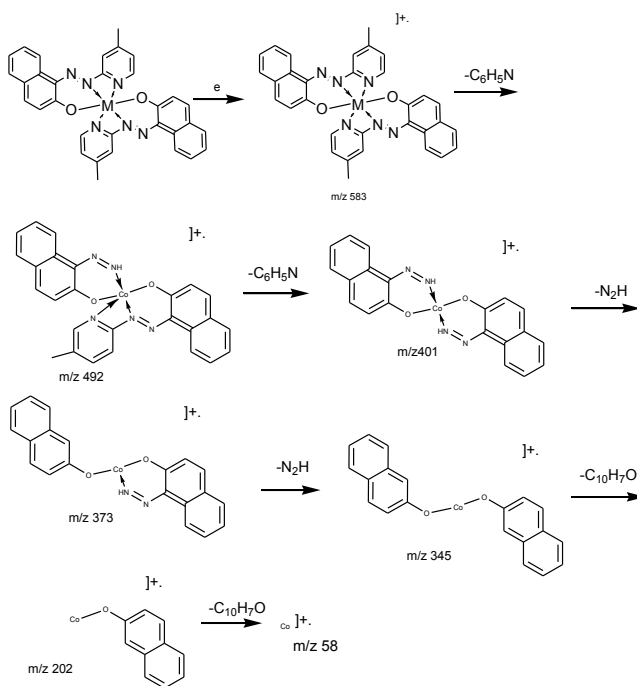

Figure 4. The fragmentation pattern of the Co(II) complex

as depicted in the Graph 13. The map also gives information regarding charge distribution and charge related properties of the molecules. The MEP was calculated using BLYP method using 3-21(d-p) basis set. The red colour of the map reflects the reactive sites of electrophilic attack and the blue colour indicates the reactive sites of nucleophilic attack. It was seen from the map that negative region (red colour) is found over nitrogen atoms of the azo group, N- atom of the pyridine and oxygen atom of napthol, while blue region is localised over the ring H atoms of the aromatic rings. Hence, the metal ion is coordinated with the azo nitrogen, pyridine nitrogen and napthyl oxygen of the ligand.
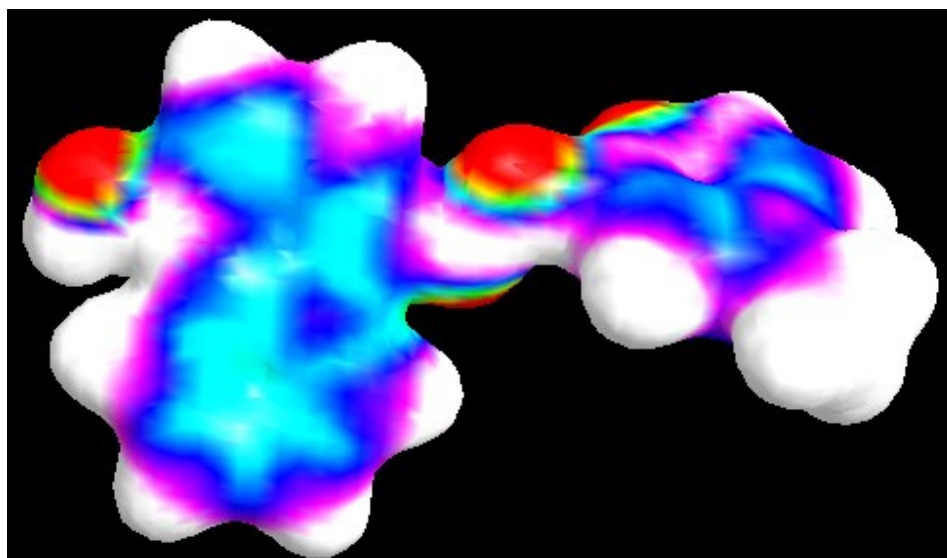
Graph 13. Electrostatic potential map of the ligand

Natural atomic charge

The distribution of atomic charges plays an important role in predicting many electronic properties such as dipole moment, molecular polarisability. The natural atomic charges of the ligand is computed and given in the table 6. The O and N atoms of the ligand are more electronegative atomic charge but the O atom is more electronegative than the N atoms that make the ligand polar with dipole moment 4.88 Debye. The pyridine-N atom is more electronegative than the azo nitrogen atoms, while the napthyl O is more electronegative than the N atoms. The ring carbon atoms attached to N and O atoms that is C1, C10, C13,C5 are electropositive while other carbon atoms are electronegative, all the hydrogen atoms are electropositive.

Table 6. The natural atomic charges of the ligand

Bond	charge	Bond	charge	Bond	charge	Bond	charge
C1	0.6235	N8	-0.3337	C16	-0.2068	H23	0.2586
C2	-0.2878	N9	-0.3630	C17	-2.2304	H24	0.2309
C3	0.0006	C10	0.2398	C18	-0.1852	H25	0.2191
C4	-0.3266	C11	-0.1702	C19	-0.0679	H26	0.2296
C5	0.1322	C12	-0.2544	O20	-0.7319	H27	0.2870
N6	-0.6810	C13	0.4179	H21	0.2549	H28	0.2687
C7	-0.5934	C14	-0.1215	H22	0.2409	H29	0.2168

Chemical reactivity

The energies of frontier molecular orbitals are useful for predicting the reactivity of the studied compounds. The energies of HOMO (Highest occupied molecular orbitals) and LUMO(Lowest unoccupied molecular orbitals) can be utilised to calculate various reactive descriptors such as electronegativity(X), chemical potential (μ), chemical hardness (η), global softness(S) and global electrophilicity index(ω).

$$X = \frac{I + A}{2}$$

$$\mu = -X = -\frac{I+A}{2}$$

$$\eta = \frac{I-A}{2}$$

$$S = \frac{1}{2\eta}$$

$$\omega = \frac{\mu 2}{2\eta}$$

The electronegativity measures the tendency of a system to attract electrons in a chemical bond, whereas the electrophilicity measures the stability of a system when it acquires additional electronic energy from the environment. It contains both the information of electron transfer that is chemical potential and stability that is the hardness (Parr & Pearson, 1983). The chemical hardness measures the resistance of a system towards the deformation of its electron cloud under small perturbation received during chemical reaction. It is seen from the electronic parameters and global reactive descriptors given in the Tables 7 and 8 that metal complexes are more reactive than the free ligand and the reactive order of the metal complexes follows the order $[NiL_2] > [CuL_2] > [CoL_2] > [ZnL_2]$.

Table 7. Electronic parameters of the ligand and complexes in *eV*

comp	*EHOMO*	*ELUMO*	*ΔE*	*I*	*A*
LH	-7.9006	2.1479	10.0485	7.9006	-2.1479
[CoL2]	-6.1752	0.4694	6.6446	6.1752	-0.4694
[NiL2]	-5.5443	-0.5711	4.9732	6.3083	0.5711
[CuL2]	-6.8226	0.4710	7.2936	5.5206	0.4710
[ZnL2]	-6.8305	1.5588	8.3893	6.9847	-1.5588

Table 8. Global reactive descriptors of the ligand and complexes

comp	*μ*	*n*	*w*	*s*
LH	5.0242	2.8663	0.823	0.099
[CoL$_2$]	3.3232	2.8529	1.224	0.150
[NiL$_2$]	2,4886	3.0577	1.878	0.201
[CuL$_2$]	3.6468	3.1758	1.328	0.137
[ZnL$_2$]	4.1946	2.6358	0.828	0.119

Table 9. Selected bond angle of the metal complexes

Bond angle	[CoL$_2$(H$_2$O)$_2$]	[NiL$_2$(H$_2$O)$_2$]	[CuL$_2$(H$_2$O)$_2$]	[ZnL$_2$]
N(6)-M(41)-N(7)	68.275	71.998	72.155	63.607
N(6)-M(41)-O(20)	109.470	88.189	89.282	59.664
N(6)-M(41)-N(26)	68.136	92.226	90.948	117.673
N(6)-M(41)-N(27)	131.331	98.977	100.709	110.991
N(6)-M(41)-O(40)	116.219	168.718	168.575	115.842
N(7)-M(41)-O(20)	104.784	91.801	88.195	27.999
N(7)-M(41)-N(26)	120.254	99.069	102.152	113.72
N(7)-M(41)-N(27)	129.589	167.388	170.887	158.048
N(7)-M(41)-O(40)	60.371	96.803	96.524	126.007
O(20)-M(41)-N(26)	127.146	168.702	169.199	141.630
O(20)-M(41)-N(27)	107.354	96.789	97.520	168.021
O(20)-M(41)-O(40)	117.807	93.655	91.945	100.862
N(26)-M(41)-N(27)	64.483	71.989	71.829	47.883
N(26)-M(41)-O(40)	108.205	88.141	89.966	111.998
N(27)-M(41)-O(40)	70.488	91.864	90.935	75.886

Table 10. Selected bond lengths of the ligand and its metal complexes

Bond (Å)	Ligand	[CoL$_2$(H$_2$O)$_2$]	[NiL$_2$(H$_2$O)$_2$]	[CuL$_2$(H$_2$O)$_2$]	[ZnL$_2$]
N(8)-N(9)	1.228	1.362	1.292	1.417	1.314
C(5)-N(6)	1.352	1.412	1,339	1.367	1.354
N(28)-N(29)	-	1.353	1.307	1.410	1.216
N(28)-C(21)	-	1.441	1.498	1.444	1.455
C(31)-O(40)	1.365	1.360	1.331	1.349	1.334
N(29)-C(30)	-	1.289	1.369	1.357	1.364

The geometrical parameters of the ligand and complexes are calculated from the optimised geometry and given in the Tables 9 and 10. It has been seen from the table that the bond angles around Co(II), Ni(II), Cu(II) and Zn(II) are close to 90^0, hence distorted octahedral geometry may be suggested for the metal complexes.

Conclusion

The tentative geometry of the metal complexes is suggested to be octahedral on the basis of the study of various physic-chemical, spectral and computational methods. The spectral data as collected experimentally were in good agreement with the computationally generated spectral data. The ligand behaves as a tridentate ligand with the N, N, O donor atoms which is confirmed from the analytical, spectral, MEP and natural atomic charge studies.

REFERENCES

Adsule, S., Barve, V., Chen, D., Ahmed, F., Dou, Q.P., Padhye, S. & Sarkar, F.H. (2006). Novel Schiff base copper complexes of quinoline-2-carboxylaldehyde as proteasome inhibitors in human cancer prostate cells. *J. Med. Chem*., *49,* 7242 – 7246.

Anitha, C., Sheela, C.D., Tharmaraj, P. & Sumathi, S. (2012). Spectroscopic studies and biological evaluation of some transition metal complexes of azo Schiff base ligand derived from (1-phenyl-2,3-dimethyl-4-aminopyrazole-5-one) and 5-((4-chlorophenyl) diazenyl)-2-hydroxybenzaldehyde. *Spectrochim. Acta A, 96,* 493 – 500.

Becke, A.D. (1993). Density funtional thermochemistry – III: the role of exact exchange. *J. Chem. Phys.*, *98,* 5648 – 5652**.**

Benial, A.M.F., Ramakrishnian, V & Murugesan, E. (2000) Single crystal EPR of $Cu(C_5H_5NO]_6(BF_4)_2$: an example of admixed ground state. *Spectrochim. Acta A, 56,* 2775 – 2781.

Dholakiya, P.P. & Patel, M.N. (2002). Preparation, magnetic, spectral, biocidal studies of transition metal complexes with 3,5-dibromosalicylideneaniline and neutral bidentate ligands. *Synthesis & Reactivity Inorganic & Metal-Organic Chem., 32,* 819 – 829.

Dutta, R.L. & Syamal, A .(1993). *Elements of magnetochemistry*. New Delhi: Affiliated East – West Press.

Galić, N., Malković-Čalogović, D. & Cimerman, Z. (1997). Structural characteristics of N,N'-bis(salicylidine)-2,6-pyridine diammine. *J. Mol. Struct., 406*, 153 – 158.

Guha, D., Mandal, D., Koll, A., Filarowski, A. & Mukharjee, S. (2000). Proton transfer reaction of a new ortho hydroxy Schiff base in protic solvents at room temperature. *Spectrochim. Acta A,56,* 2669 – 2677.

Hallas, G.& Choi, J.-H. (1999). Synthesis and properties of novel aziridyline azo dyes from 2-aminothiophene- part 2:application of some disperse dyes to polyester fibres. *Dyes & Pigments, 40,* 119 – 129.

King, R.B. & Bisnette, M.B. (1966). Organonitrogen derivatives of metal carbonyls. 1: reactions between metal carbonyl anions and haloalkyl amines. *Inorg. Chem., 5*, 293 – 300.

Lever, A.B.P. & Solomon, E.I. (2014). *Inorganic electronic structure and spectroscopy.* Hoboken: John Wiley & Sons.

Nakamoto, K. (2009). *Infrared and raman spectra of inorganic and coordination compounds – part A: theory and application in inorganic chemistry.* Hoboken: John Wiley & Sons.

Parr, R.G. & Pearson, R.G. (1983). Absolute hardness: companion parameter to absolute electronegativity. *J. Amer. Chem. Soc., 105,* 7512 – 7516.

Saxena, A. & Tondon, J.P. (1984). Structural features of some organotin(IV) complexes of semi- and thio-semicarbazone. *Polyhedron, 3,* 681 – 688.

Shakir, M., Mohammed, A.K. & Nasman, O.S.M. (1996). Transition metal complexes with 16-18 membered tetrazamacrocycles bearing polyamides gropups. *Polyhedron, 15,* 3487 – 3492.

✉ **S.N. Chaulia**
Department of Chemistry
G. M. University
Sambalpur, Odisha (India)
E-mail: satyanarayanchaulia@gmail.com